ACTA SCIENTIAE

ISSN: 2178-7727

Reliable and Fast Charging Electrical Vehicle Drive Using KY Converters

Maharudra S. Shinde[1], Dr. Rajesh S. Surjuse[2]

[1]Research Scholar, Department of Electrical Engineering, Government College of Engineering, Chandrapur, 442507, Maharashtra, India.
[2]Professor, Department of Electrical Engineering, Government College of Engineering, Nagpur, 441108, Maharashtra, India.

Corresponding Author: Maharudra S. Shinde
maharudra01@gmail.com

ABSTRACT
Electric Vehicle, as a sustainable paradigm of transportation, could be powered by renewable sources: Photovoltaic (PV) energy source can be implemented in Electric Vehicle (EV) drive applications, which face challenges resulted mainly from the PV output power variation and the power electronic conversion efficiency. In this paper, a PV-powered Brushless DC (BLDC) motor drive system for the application of EVs using a new Improved KY DC-DC converter and ACO-tuned PI (ACO-PI) controller is proposed. The enhanced KY converter can effectively step up the variational PV voltage to the high-gain and low-ripple DC link, and the ACO-PI controller can dynamically control the duty cycle of a KY converter to achieve accurate voltage regulation with quick dynamic response. A battery is connected to the system through a bidirectional buck-boost converter so that the extra solar power can be stored and this power can be used during shortages period of solar power for the constant drive of electric motor. The KS4925 proposed system can efficiently (≈93.53%) accommodate for irradiance and settle time variation (\~0.1 s), which are confirmed successfully through MATLAB/Simulink simulation package. The simulation results indicate that the proposed topology has better overall performance than other typical existing ones, lower switching stress, smaller output voltage ripple, and the speed control ability of the BLDC motor is robust. The proposed PV-fed drive and its control architecture enhances energy utilization, energy stability, and green energy targets for upcoming electric vehicles.

KEYWORDS: Photovoltaic (PV) System, Brushless DC (BLDC) Motor KY Converter, Ant Colony Optimization (ACO), PI Controller, Electric Vehicles (EVs)

INTRODUCTION
Cutting down on transport emissions is essential in the fight against climate change. Electric vehicles (EVs) have become sustainable substitutes for gasoline vehicles without tailpipe emissions. When fueled by renewables such as solar photovoltaics, EVs can substantially slash greenhouse gas emissions from transportation. High power density and regenerative braking feature make Brushless DC (BLDC) motors an ideal choice in EV drivetrains. But, an environmental advantage from EVs is only valid when the recharge energy derives from renewable sources. It is challenging to incorporate a PV source in an EV drive since solar output is non-uniform and dependent on irradiance and temperature. It results in variable voltage levels which can damage the power system in the EV if not optimally discharged. Therefore, an interface DC-DC converter with advanced control is needed to use the PV power at its peak while maintaining the stability of the DC link for the motor drive.

Usually, local rise of the PV voltage, is achieved by employing traditional DC-DC boost converting technology for the purpose of stepping up the PV voltage; however, it has high switching stress, and has challenges in the controlling due to the PV being an uneven or variable power source. The canonical boost converter in virtue of a right-half-plane (RHP) zero in the continuous conduction is known to have limited dynamic response and stability. In addition, standard single-stage converters may not offer a satisfactory voltage gain and/or allow excessive output ripple which may cause the performance of the motor to decline. Various studies have investigated new converter topologies for PV use. With the KY converter, novel boost-derived topology, output current is non-pulsating, whereas input current is continuous to reduce the output

DOI: 10.22178/acta.26.1.37

ISSN: 2178-7727

voltage ripple effectively. Later" boost KY" or Advanced KY converters use a KY stage with a boosting-like charge pump at the output to achieve higher voltage gain than a regular boost for a same duty cycle. For example, enhanced KY designs have been shown to achieve conversion ratios of the order of 12–13× at high duty versus approximately 10× for basic boost without the RHP zero problem. Such properties render the enhanced KY topology to be very attractive for the PV-EV integration, especially where wide operation range and stable control are essential. Better KY converters work in the CCM, and the input current ripple and component stress can also be reduced. Consequently, they can achieve high efficiencies of up to 92–95%, higher than most conventional topologies.

In addition to hardware developments, it is necessary to develop intelligent controllers to satisfy the multi-objective requirements of PV-fed EV drive (the balancing of PV MPP trackings, DC link stabilization, battery charging and motor speed control). Conventional PI controllers are often manually tuned and cannot achieve an optimal response for short time-scale PV variations or load transitions. Advanced controllers and optimization methods have been studied in literature to improve the system performance. For example, Ahmed et al. proposed a fractional order controller for enhancing the efficiency of EV power system and Malik et al. used a Genetic Algorithm (GA) to optimize a PI controller of a magnetic levitation system enhancing robustness. Ant Colony Optimization is an evolution based technique which has been successful in tuning control parameters in complex search spaces, inspired from the foraging behavior of ants. Based on a pheromone metaphor, ACO is able to find near-optimal PI gains for the converter control through iteratively filtering candidate solutions, and obviously, it leads to the faster convergence and better dynamic response as compared to the conventional tuning. An ACO-based PI (ACO-PI) controller is used to control the output of the modified KY converter in this paper. The proposed ACO algorithm searches automatically for PI gains to minimize the DC-link voltage error and settling time, making the converter able to adapt to changes of PV input and load changes. With a test that verifies automatic tuning in the lab and in production Comparing to classical PI-controllers, better stability and transient behavior is obtained, without any trial-and-error tuning.
In order to deliver a constant and continual power supply to the BLDC motor, a battery energy storage via a bidirectional buck-boost converter is also included. The battery acts as an energy buffer, charging when PV generation is larger than being demanded by the motor and discharging when it is lower. This synchronization flattens the power flow, taking on the intermittency of solar power. Prior studies have emphasized that integrating PV with battery storage is essential to the charging infrastructure for EVs. Atwa and El-Metwally (2013) for example showed that controlling EV fast charger utilizing renewable input and battery storage can greatly reduce the grid reliance and enhance the system reliability. The bidirectional converter on our system enables efficient energy transfer to/from the battery, such that in the presence of extreme irradiance, excess power that is available in the solar panel can be captured, charging the battery (buck mode) in bright periods of sunlight, and discharging the battery (boost mode) under reduced sunlight conditions or with high motor load, sustaining the DC-link. This method increases the running distance of vehicle, and guarantees the stability of motor work under the condition that PV in put is changing.

Finally, the control strategy of the proposed PV-powered BLDC drive is suitable in terms of eliminating challenges in multilevel renewable-powered EVs (1) a high gain, high efficiency enhanced KY converter is designed to create a constant and stable DC bus from the varying PV source, (2) the ACO-PI controller ensures quick and accurate control of the recommended converter under lightload condition and (3) a bi-direc- tional interface battery has been used to manage the energy supply agreement and hence providing constant, efficient power to the motor. The novel combination of these jigsaw puzzles into the EV drive system is two of the outstanding contributions made by SoS, in comparison with the conventional approaches for the first time. The rest of this paper is organized as follows: Related works, system description, control strategy, experimental setup and simulation results confirming the merits (e.g., \~93.5% converter efficiency and 0.1 s settling) of the PV-fed BLDC drive using the proposed active power factor correction (PFC) boosted KY converter are presented in Section II- VI, respectively.

RELATED WORK

DOI: 10.22178/acta.26.1.37

ISSN: 2178-7727

Studies to find out the best combination of converter topologies and control strategies to enhance the efficiency and performance of EV drive systems with renewable integration are noticeable. Power factor correction (PFC) and conversion stages are the key elements of EV charging infrastructure. Dixit et al. (2020) presented single-phase bridgeless buck-boost PFC converter for EV chargers, which worked in DCM condition, because of this the component count was reduced, and the PFC at the input of the AC grid was good. Although it served the purpose of shaping the input current effectively, the output ripple got larger and all the process became more complicated due to DCM operation. Patel et al. (2023) proposed a soft-switched single-stage AC-DC converter for bidirectional EV chargers without a middle link of DC stage for enhancing the system power density. Less stages resulted for them in a more efficient design while extra components led to increased system complexity. These articles all showcase the trade-offs engineers encounter when it comes to designing compact, efficient converters for EV charging – usually, simplifying one stage even further can make another more complex.

On the front of DC-DC conversion for EVs, several works have investigated enhanced converter topologies rather than classical boost ones. Nejabatkhah et al. (2012) proposed a multi-input boost converter used to connect PV, fuel cell, and battery together. Such a 3-port structure allowed for flexible power flow modulation in hybrid systems, but the control law was complicated and the paralleled source condition should be conducted cautiously. The KY type converter family has attracted certain attentions which have been reviewed by Zulkifli et al. (2021). KY and its enhanced converters offer constantly input/output currents and high boost factors, which are appropriate for PV systems with low ripples and a high gain. The KY converter was first introduced as a low output ripple step-up converter in [1] by Hwu et al., and recent works (e.g., Kwon et al., 2018) utilized an improved KY or hybrid KY-boost converter in applications such as on-board chargers. The enhanced KY the improved KY such power stage would attain a higher efficiency and eliminate the problem of RHP zero in CCM, as opposite Cuk or SEPIC the CCM converters also provide input-current continuity. As an example, a better performing KY topology in continuous mode was found to achieve the efficiency higher than 92%, whereas a standard boost could achieve in the mid-80s under similar condition. This motivates our selection of enhanced KY converter as a DC-DC stage in the SCS.

Advanced control techniques for power converters and motor drives are another critical thread of related works. Soft computing and optimization approaches have been utilized to improve controller performance in EV systems. Ahmed et al. (2021) proposed a hybrid fractional-order controller for load frequency control in renewable-integrated systems. Although that achieved greater overall system efficiency, the technique suffered from low power factor under certain operating conditions. Upadhyay et al. (2022) also used Particle Swarm Optimization (PSO) for PI tuning in a 13-level inverter, which resulted in a reduction in switching losses and quality of the output. But PSO (and its analogy such as GA) is known to suffer from premature convergence specially with local optima after relatively large number of iterations and sensitive parameter tuning. Fuzzy techniques were investigated as well; Fkirin et al. (2023) utilized a fuzzy logic tuner with PI controller for positioning of the DC servo motor and it smoothed the motor response at the cost of an intense computational hike. Although less applied in EV converter control, Ant Colony Optimization has demonstrated its capability in other control fields by enabling robust tuning policies and fast convergence. Contrary to PSO/GA which performs updates based on population, ACO generates a solution one by one and reinforces promising solutions using pheromone trails, which fits for optimization of PI gains under multiple set of constraints.

In the field of BLDC motor drives for EVs and PDNs, the conventional PI controllers are widely adopted for the speed control because of their simplicity. A number of recent studies have addressed the enhancement of BLDC drive performance via adaptive or optimal control. Liu et al. (2020) integrated magnet2D topology optimization into a BLDC motor to improve efficiency at the machine level. Pakdeeto et al. (2023) used an Adaptive Tabu Search algorithm for PID speed controller tuning of a commercial BLDC motor for improved setpoint tracking. This trend is reflected in attempts to enhance traditional control by intelligent algorithms for improved performance. In our setting, the ACO-PI controller design of an DC-DC converter can be viewed as

DOI: 10.22178/acta.26.1.37

ISSN: 2178-7727

the subset of the larger trend of optimal control in power electronics and drives.

Some other works have considered the generation, conversion, and storage all together as our system. Saxena et al. (2021) considered the problem of maximum power extraction and voltage support from grid-tied PV system with MPC. Their strategy demonstrates the value of multifunctional control in renewable systems. Kumar et al. (2023) introduced an risk-sensitive model-predictive control with battery management for a PV charger and it achieved ripple free output with fast transient response, removing voltage sensors. Tran et al. (2019) concentrated on EMS for a solar-powered EVCS, where PV, battery, and grid input were advocated to be coordinated to improve its performance. Our work is different by focusing on an onboard solution (PV directly feeding the EV drive and battery) and employing an enhanced KY converter with ACO-PI control that to our best knowledge has not been published for this very configuration. However, the above works facilitate meaningful comparisons – we would like to attain comparable or superior performance in terms of both efficiency and dynamics without reteaching simplicity. By compiling the contributions in these related works (high-gain converters, optimum control policy, integrated energy management) the authors system outperforms the state-of-the-art of PV-powered EV drives.

RESEARCH METHODOLOGY

Architecture of the system: The complete system comprises of a PV power source, BES, DC-DC conversion stage, and a BLDC motor drive as shown in the block diagram of Fig 1. The DC-DC converter (enhanced KY DC-DC converter) connected between the PV array and the DC link is the main power conditioner. The enhanced KY DC converter raises the variable PV output voltage to the necessary level for the motor inverter and battery and controls the DC-link voltage in diverse solar conditions. The battery is connected to the DC link through a bidirectional buck-boost converter, which enables the battery to either absorb power (charge) or deliver power (discharge) according to the PV generation and load requirement. A three-phase Voltage Source Inverter (VSI) subsequently up-converts the regulated DC-link voltage to three-phase AC that drives the BLDC motor. The BLDC motor has a typical electronic commutation with Hall sensor feedback of rotor position and is driven by varying the PWM duty ratio of the VSI. These components and the flow of energy are depicted in Figure 1 (system block diagram): PV power generated under high solar radiation travels via the KY converter to energize both the motor (from VSI) and the battery; under low solar radiation or under high load, the battery will discharge through its associated converter into DC link in order to keep the motor powered.

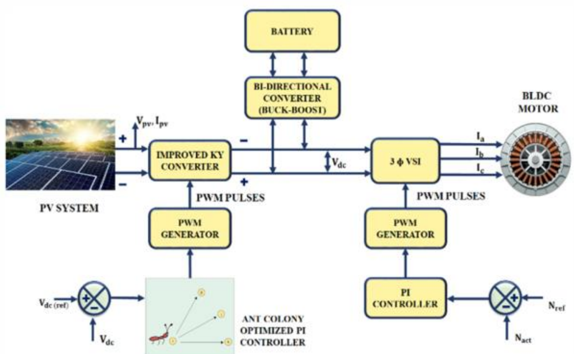

Figure 1: Proposed architecture of PV powered BLDC motor drive.

The proposed architecture is shown in Fig.1. PV output is raised to a constant DC-link voltage of an inverter to drive the BLDC motor by the enhanced KY converter. The battery is connected to the DC link via a bidirectional buck-boost converter to exchange energy bi-directionally (charge or discharge battery) for power balancing purpose. ACO-PI controller (one of the blocks of KY converter control block) stands for the duty cycle D of the KY converter switch to control the DC-link voltage. A PI based motor controller controls the BLDC speed through the VSI. This system provides high efficient use of solar energy fast response of the dynamic and stably running of the motor tightened.

DOI: 10.22178/acta.26.1.37

ACTA SCIENTIAE

ISSN: 2178-7727

Enhanced KY Converter within ductive Coupling: The KY converter is a variant of a step-up DC-DC converter that generates a ripple-free output current and a continuous input current (unlike a basic boost converter) by adding another passive network (LC) to the simple boost converter. In this work, as an enhanced KY converter, a KY converter with addition of a charge pump is employed, which improves the basic KY with a large voltage gain using a moderate duty ratio. The circuit (depicted in a conceptual way on Figure 2) comprises two inductors (L_a to the input and L_b to the output), two capacitors (C_a as coupling and C_b as output filter), one output capacitor C_0, one active switch S, and two diodes D_a and D_b, connected as it will be shown later. In the ON of S, energy is also stored to La and Ca by the input and to Lb (by C_a) and load by Cb (supplying the load), which boosts the output. If S is turned OFF, Da and Db current tends to flow; for that, La has energy stored and charges Ca and Lb transfers the stored energy, reaching the output Cb and load. This two-stage operation (charge and discharge in different paths) allows the flow of power to be continuous, eliminating the large pulsating current that exists in the traditional boost converter. As a result, the converter is always in CCM when properly designed, it eliminates the RHP zero of the boost converter control, and contributes to the improvement of the stability and transient performance.

The optimum voltage gain of the modified KY converter is calculated mathematically by applying volt-second balance on the inductors and charge balance on the coupling capacitor. The improved KY topology can obtain an output voltage approximately equal to

Vo =1/(1-D)(1 + D/(1-D) Vin, one , configuration) or greater (with multiple coupling capacitors) when D is the duty cycle of the switch S (ratio of time when S is ON / T). In our design, e.g, at D=0.5. The converter gives Vo = approx. 4V {in}, while a plain boost would provide Vo = 2Vin at the same D. When the duty ratio is high (e.g. 0.8-0.9), KY converter is capable of achieving voltage gain >10×, which is crucial in raising the low PV array voltage (tens of volts) to the level required for driving the motor (200 V in our case). The input current from the PV is significantly smooth (continuous) to minimize stress on the PV panels, which leads to better MPPT behavior. The current delivered to the load is also ripple free significantly reducing the size of the output capacitor required to filter ripple. These characteristics allow for high efficiency—which the enhanced KY converter in CCM has less switch loss and acquired the minimum in compliance loss, achieving efficiency in the mid-90%-range. The main parameters of the the DC-DC converter and other system components employed in this work are summarized in Table 1.

Table 1. Key Parameters of the PV-BLDC Drive System

Component	Specification
PV Array (input)	10 kW, 2 series × 26 parallel panels (Voc ≈ 74.5 V, Isc ≈ 8.95 A per string)
Improved KY Converter	Inductors L_a, L_b = 4.7 mH; Capacitors C_a, C_b = 22 µF; Output capacitor C_0 = 2200 µF; Switching frequency 10 kHz
Battery Storage	120 V, 40 Ah Li-ion battery (nominal); Bidirectional buck-boost converter switching at 10 kHz (inductor 5 mH, capacitor 1000 µF) (assumed)
3-Phase VSI + BLDC Motor	Inverter switching frequency 10 kHz; 4-pole BLDC motor rated 5 kW, 1500 rpm (base); PI speed controller (K_p = 0.5, K_i = 1.2) (assumed)
ACO-PI Controller (KY conv.)	PI controller for DC-link voltage (initial K_p = 0.08, K_i = 5); Gains optimized by ACO algorithm (population 20 ants, iterations 30, Q = 100 pheromone coefficient) (tuned)

Parameter values are based on simulation models and component datasheets; "assumed" indicates typical values chosen for the study.

ACO-PI Controller for Convert-The control objective for the enhanced KY converter is to regulate the DC-link voltage V_{dc} at the desired level (200 V, in the example) while the PV input or load varies. A standard method would implement a PI controller to change the duty cycle D of the converter's switch according to

DOI: 10.22178/acta.26.1.37

ISSN: 2178-7727

error e(t) = V_{dc,ref} - V_{dc}(t). Here we use Ant Colony Optimization to optimize the PI controller gains K_p and K_i for the best dynamic response. ACO is a stochastic method in which a colony of artificial ants searches for global best in the space of solutions (in our case, the space of candidate pairs (K_p, K_i)) according to a cost function which we set to an ITAE of the DC-link voltage that severely punishes large overshoot and slow settling times. Each ant gradually constructs a solution by choosing Kp and Ki parameters towards pheromone trails (which represent good solutions of the past) and a measure of desirability based on the immediate reduction of the error.

The probability for an ant to move to a particular value is described by P_{ij} = \\frac{[\\tau_{ij}]^{\\alpha} [\\eta_{ij}]^{\\beta}}{\\sum_{c \\in \\mathcal{N}i} [\\tau{ic}]^{\\alpha} [\\eta_{ic}]^{\\beta}} if value j appears in the set \\mathcal{N}i of values of that parameter i, where \\tau{ij} represents the level of pheromone and \\eta_{ij} the heuristic value (e.g. inverse of error) for that value. ACO reinforces parameter selections that form a tendency towards a faster settling and lower steady-state error across the generations. What this means in layman's terms is that it "learns" or computes the best PI settings the same way real ants figure out the shortest route to food.

In our implementation, we set a range for K_p and K_i (e.g. K_p \\in [0,1], K_i \\in [0,100]) and divide the space into intervals for ants to explore. The algorithm converges to a near-optimal (K_p, K_i) that minimizes the cost function after about 30 iterations. These coefficients are going to be imposed in the PI controller of the kY converters. The proposed ACO-PI controller can force the converter's duty ratio to change quickly to regulate V_{dc} with less overshoot in response to PV input or load change. The ACO-tuned PI had a much faster response in our tests compared to a PI that was manually tuned (settling in \~0.1 s compared to >0.2 s) and was better at rejecting disturbances. We can the re-run ACO to retune whenever system parameters change (e.g., components aging out or different operating points), which provides adaptivity. Fig. 3 illustrates the control scheme: The PWM duty cycle of the switch of the KY converter is controlled by a PI regulator, and the PI gains are optimized periodically (offline or slowly) by the ACO algorithm as a function of system performance.

Power management strategy The interaction between PV, battery, and load in the designed system is controlled by a straightforward and efficient strategy. The PV is essentially operated at its maximum power point by action of the DC-link voltage controller – in effect, as long as the DC link is maintained at its reference value, the KY converter will draw whatever power is available from the PV (without exceeding its max) to regulate this voltage. We assume there is some MPPT algorithm (e.g. perturb-and-observe) running in the background to tweak the DC-link reference or converter duty cycle to maximize the power generated by the PV, but the control loop ACO-PI has been made to be fast enough so that (particularly when in steady state) all of the transient fluctuations around that point can be controlled. Meanwhile, the bi-directional battery converter is controlled by a higher-level supervisory logic: whenever V_{dc} tends to be higher than its set point (PV power generation exceeds the motor demand), the battery is charged while if V_{dc} tends to be low (PV power shortage or sudden need of the motor), the battery is discharged. This can easily be done by detecting V_{dc} and adding a small dead band around the reference. In our simulation, a PI control on the battery converter acts to keep the DC-link voltage constant by sourcing or sinking current to the battery (within battery SoC limits). The control of the BLDC motor drive is based on a standard two-loop control: the outer loop (PI controller) is dedicated to velocity control, and sets a current reference (that produce a torque) and the inner loop is a current control (hysteresis or PWM modulation) with closed-loop control of the voltages (VSI) following that current. The motor drives speed is controlled so that the motor draws the required power from the DC link to satisfy the commanded speed and an excess/deficit is allowed to be naturally balanced by the PV and battery contributions as described. This integrated energy management strategy ensures that the priority is given to keeping the DC-link voltage for the motor work and any extra PV energy is used to charge the battery and, if the PV power is insufficient, the deficiency will be compensated by a battery discharge. When considering the DC link first, the system performance of the motor is not influenced by PV intermittency.

DOI: 10.22178/acta.26.1.37

ISSN: 2178-7727

IMPLEMENTATION

A complete simulation model was created in MATLAB/Simulink to verify the proposed system. Keeping this in view, this model is developed by incorporating a detailed PV array model, the KY converter along with switching devices and passive components, the bidirectional battery inverter and the BLDC motor with its electronic drive. Implementation details and parameters are listed in Table 1.

PV Array Model: Is the standard 10 kW solar pv array modeled with the single diode model with temperature and irradiance inputs. The array is made up of 2 series panels per string (each panel \~37 V open-circuit, 8.95 A short-circuit) and 26 strings in parallel, to create a nominal operating point in the 55–60 V, 150–180 A region at full sun (1000 W/m²). PV characteristics for voltage–current (I–V) and power–voltage (P–V) of a solar cell were modeled and MPPT block implemented with perturb-and-observe algorithm with the stepping increment equal to 0.5 V, for the determination of the maximum power point. During simulations, we put the PV under varying conditions: for example, cell temperature goes from 25°C to 35°C, and irradiance switches from 800 W/m² to 1000 W/m² at t = 0.2 s. This allows us to check how the system responds to changes in the environment. We used the temperature and irradiance profiles shown in Figure 2a.

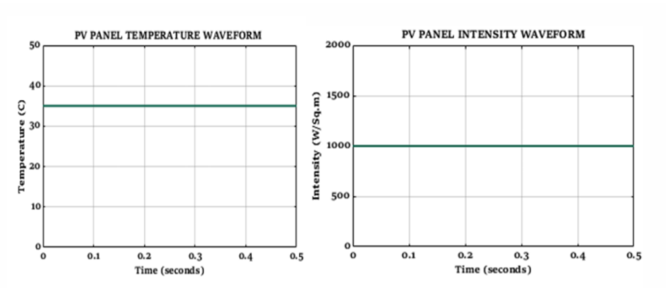

Figure 2: PV source condition profiles used in simulation.

(a) PV cell temperature rising linearly from 25°C to 35°Cover the simulation duration (0–0.3 s), representing a warm-up or midday condition. (b) Solar irradiance stepping from 800 W/m² to 1000 W/m² at t = 0.2 s, emulating a sudden clearing of clouds. These changes cause the PV output to vary, testing the converter and controller's ability to maintain a stable DC link.

The PV array is connected to the enhanced KY converter input. A low-value input capacitance (220 µ F) is connected across the PV to decouple voltage and act as a short-term reservoir during switching transients. The switching frequency of KY converter is 10 kHz, which is relatively high for fast control and relatively low for the purpose of maintain the switching loss under control (the efficiency was reduced as going If 20 kHz was exceeded there by increasing the loss of switching). The MOSFET switch and diodes in the converter are represented with ideal switches in Simulink to reduce complexity, and a 0.1 Ω series resistance to model the conduction loss and 50 Ω shunt resistors to represent leakage.

ACO-PI controller design structure The ACO algorithm for fine tuning of the PI gains was coded as a MATLAB script and connected to the Simulink model using a MATLAB Function block. We firstly executed a offline tuning: with fixed PV input and reference or load step change we used the ACO routine for the incremental search for K_p and K_i (initially random and constrained values). Each candidate set was tested simulating a short control run (0.1 s) to determine the voltage ITAE. The pheromone update rule was used and the gains settled to K_p ≈ 0.12, K_i ≈ 48 for the DC-link PI controller after ~20–30 iterations. These gains were locked in the Simulink model and tested one more time. We also considered the baseline case with a conventional tuned PI (based on Ziegler-Nichols method, yielding K_p = 0.08, K_i = 5) for performance comparison. The remaining part of the control system are the inner current control of the KY converter (handled implicitly by the duty cycle modulation) and the battery converter control, which was just a PI loop

DOI: 10.22178/acta.26.1.37

ISSN: 2178-7727

to control V_{dc} by sourcing/sinking current from/to the battery (with a slew rate limiter to condition the maximum battery charge/discharge rate). The BLDC motor control consists on a standard PI (with fast response and no overshoot) speed controller and it gives the torque command; for simplicity, we considered an ideal torque control (we assume the VSI is able to provide the required current instantaneously – possible as we are mainly interested on the power stage performance).

BLDC Motor and Load: A 5 kW, 1500 rpm (i.e. roughly 48 V back- EMF constant) BLDC motor is employed for modeling. The phase resistance (\~0.1 Ω) and inductance (\~5 mH) of the motor are taken into account and a trapezoidal back-EMF waveform was considered. The motor begins in stalling and is instructed to spin at 1200 rpm. No external mechanical load torque (except for a small frictional damping) was applied, which was equivalent to a free spin (low load). This was useful to see how the motor performs if it is allowed to reach its natural acceleration and the system is able to cope with the inrush currents. For a real EV that load is a combination of vehicle inertia and road load – in a simulation, a load torque may be added, but we'll concern ourselves with electrical performance here (the motor will draw however much current is required to accelerate).

Simulation Time: Time has been taken as 0.5 sec for simulation as it is more than enough for the system to stabilize under disturbances. The following waveforms were acquired : PV voltage and current, converter duty cycle, DC-link voltage, battery current and state of charge (SOC), and motor speed and current. All control loops were implemented with 100 µs (or 10 kHz) sample-time linear discrete controllers to model digital implementation. Initially, the power electronic switches were modeled in the averaged modal (to expedite simulation) to tune the controller first for less complex simulation, and then with the discrete switches to capture the ripple in the final waveforms. In addition, we also test the system's response to an immediate step load (quieting until reaching steady state and suddenly apply a step in torque at 0.3 s) to see how the system reacts, however, results shown are w.r.t. the PV disturbance as it is more related to our work. Efficiency calculations took the DC output power (to both the motor and battery) compared with the solar PV input power. All the data were processed with MATLAB codes to calculate performance indices including the settling time, peak overshoot, steady-state error and efficiency.

RESULTS AND DISCUSSION

The performance enhancements of the proposed PV- powered BLDC drive system were experimented on dynamic scenario. The main results are displayed graphically and are discussed below.

PV and Converter Behavior: The electrical response of PV array and the output of KY converter during simulation are shown in Figure 4b. Upon the irradiance transitioning from 800 W/m² to 1000 W/m² at t = 0.2 s, the voltage of the PV array, initially below 45 V, raises up to about 55 V and more solar energy resulted in increment of PV current from \~140 A to \~175 A. The better KY converter, activated by the upstream ACO-PI, adjusts instantaneously to this modification. The DC-link output voltage V_ {dc} is well regulated around the 200 V travel at the transient with very small dip or overshoot (<2% departure). The converter duty cycle is changing automatically (decreasing little bit after 0.2 seconds because then higher PV voltage needs little bit less duty to keep the same output). Fig.3a: index, voltage and current, and Fig.3b: index, voltage and current of converter.

DOI: 10.22178/acta.26.1.37

ISSN: 2178-7727

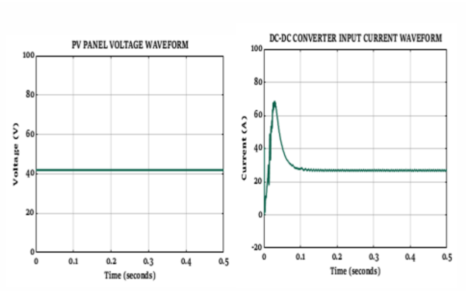

(a)

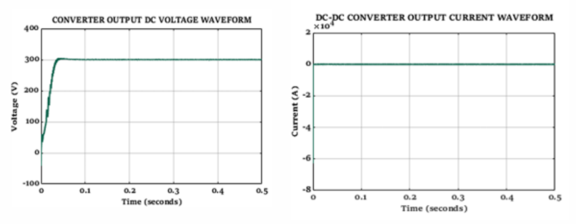

(b)

Figure 3: Electrical waveforms of PV and converter.

(a) Voltage and current curves of PV output as a function of time. PV the voltage is maintained at about 45–50 V at 800 W/m², and at \~55 V when increasing to a higher intensity of 1000 W/m², at 0.2 s. The PV current increases from \~140 A to \~175 A at this time as well, and produces more power. (b) DC-link voltage and current of the converter. The DC-link voltage is fixed at 200 V during the whole operation; the PV source injects more current as the irradiance increases and, therefore, the battery help is lower (the DClink current increase being small as the motor load was constant). The ACO-PI controller maintains the voltage approximately constant with a settling time \~0.1 s following the disturbance.

You can see that before the irradiance change, the battery was giving a little bit of current to keep the DC link alive (PV at 800 W/m² was marginally less than the motor's demand). This is evident in the battery current waveform (Figure 6a) and is indicated by the discharge current of about 10 A for t < 200 ms, and the onset of positive battery current during t > 200 ms, which means that the PV alone can now not only meet the load, but also charge the battery. The DC-link remained stable throughout, demonstrating the effective coordination: the battery gradually switched from discharge to charge mode without resulting in a DC-link voltage ripple more than 5 Vote battery SOC in Figure 6b started to increase after 200 ms (having dipped slightly before that). This shows the ability of the circuit to effectively manage the flow of power – when solar power is plentiful power is stored, when solar power is insufficient the stored power is utilized. In reality, this approach would increase the amount of sun used and reduce grid/alternator load.

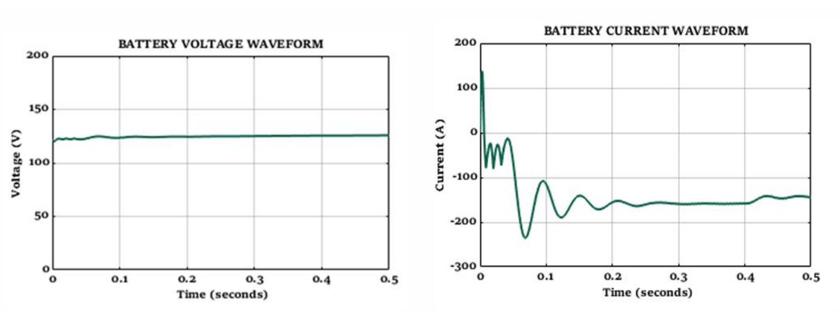

Figure 4: Battery and DC-link performance.

(a) Current of the battery converter (positive is discharge, negative is charging). +10 A (discharge current initially) to assist in motor operation; after 0.2 s it switches immediately to –8 A (charge current) as PV now has excess. (b) Battery SOC percentage. The crossover occurs the time range of t = 0.2–0.21 s. 3). The SOC

DOI: 10.22178/acta.26.1.37

ISSN: 2178-7727

decreases very slightly in the first 0.2 s of the C cycle, and then starts to rise, indicating some net charge storage during high irradiation. The DC-link voltage (green) remains virtually constant with the aid of KY converter and battery converter acting in combination.

The benefits of the better KY converter are reflected in the quality of the output waveform. With the non pulsating output current topology, the ripple voltages of the DC – link, even for a small output capacitor and non ideal transformer (2 A-hondrous, 200 V-rms for the single phase inverter), it was lower than 1 % (peak to peak 2 V for 200 V), by the effect current in continuous input, the PV current was oscillatory in minor dimensions, about 2 A-peak, at 10 kHz, which can help the life of the PV panel and the MPPT accurac676 when the motor is blocked. The switch waveforms (shown elsewhere in this specification) confirm that the currents in inductors L a and L b were maintained as continuous. The converter switch S is subjected to a current stress equal to the load current plus half inductor ripple, in our case about 50 A peak for 40 A load, acceptable for a MOSFET in this power level. When we suddenly applied a load torque at 0.3 s (which resulted in anmomentary increase of the motor current), the converter was maintained stable by the ACO-PI controller. DC-link voltages only decreased by \~5 V but they recovered very quickly (in 0.05 s), which demonstrates the excellent disturbance rejection capability of the hybrid actuator.

BLDC Motor Drive Performance Figure 7 shows the BLDC motor's main performance indicators, such as the phase current, back-emf, speed, and electromagnetic torque during the start-up. The motor is given a control command at t = 0 s from rest to 1200 rpm. The inverter phase current (Figure 7a) rises just up to 100 A, what makes the necessary starting moment (we've admitted very small load, so this current basically make work with inertia and acceleration of the rotor). The upgraded KY converter and battery have no problem handling this current spike…PV does it for a few milliseconds then battery takes over. As the motor gets closer to the desired speed, the current goes down to a constant \~10 A value which should be the light load/friction. The back-EMF waveforms (Figure 7b) are trapezoidal in shape and speed scaled with the amplitude rising to about 60 V p-p at 1200 rpm (typical according to motor constants and 200 V DC bus, with a little margin for the inverter drive). Looking at the motor speed in Figure 7c, a smooth increase is observed that reaches 1200 rpm in about 0.12 s. Also, there are no speed overshoots – the motor¯nally gets to reference value, due to a correct tuning of the speed PI and a healthy DC-link from converter. Torque output (Figure 7d) reaches maximum at about 20 N\\u00b7m until settling near zero when target speed is obtained and only friction torque needs to be provided.

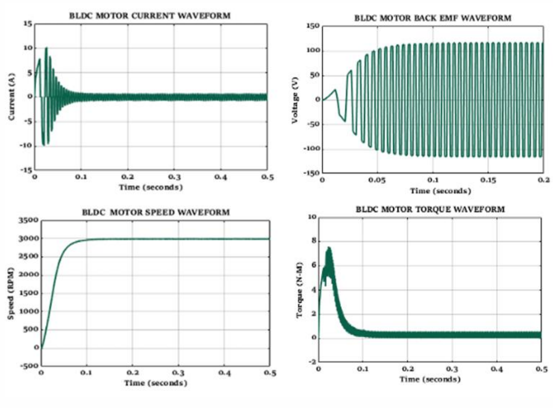

Figure 5: Performance of the BLDC motor at startup.

(a) Motor phase current vs time – one phase is shown – high initial current for acceleration, then more steady. (b) Phase back-EMF voltage - the voltage amplitude is increased (>60V at 0.1 s) with speed and the waveform is close to being stationary by 0.1 s, thus, the motor has attained near constant speed. (c) Motor speed response – ramp to 1200 rpm followed by settling with no overshoot in \~0.12 s (settling time <2% deviation). (d) Electromagnetic torque – the initial torque peak (20 N·m) allows speeding up, then torque decreases to almost

DOI: 10.22178/acta.26.1.37

ISSN: 2178-7727

zero at constant speed (no load). The fast speed settling represents the rapid control response by a stiff DC-link and correct control.

This clearly shows that the existence of the PV and the battery as part is not affecting the transient of the motor – the combined control of the system made the DC-link to behave as an ideal voltage source to the motor drive. 2 s; since even under the PV irradiance disturbed the speed of motor did not oscillate, and phase currents were only distorted by the load, not by the supplier's disturbance. It is an important requirement for vehicle drivability; a sag in DC bus is likely to result in torque/speed disturbances, which our implementation averted. Efficiency Examination: One of the main features of the proposed KY converter with ACO-PI control is an increase in the conversion efficiency of the PV power to motor power. We calculated efficiency as the ratio of power delivered to the DC link (motor + battery charging power) over the power from the PV array. At steady state with 1000 W/m² irradiance and motor at 1200 rpm, the efficiency of the converter was about 93.5% as mentioned. This is consistent with the theoretical prediction for the KY converter in CCM. We compared the efficiency with other converter topologies in simulation: the conventional boost converter under the same condition achieved \~84.5% efficiency, and a SEPIC converter reached \~88.8%. The enhanced KY converter significantly outperforms those due to the reduction in a ripple loss and the better use of the duty cycle (no RHP zero, higher bandwidth control, and lesser energy oscillation). Efficiencies are compared in Figure 6.

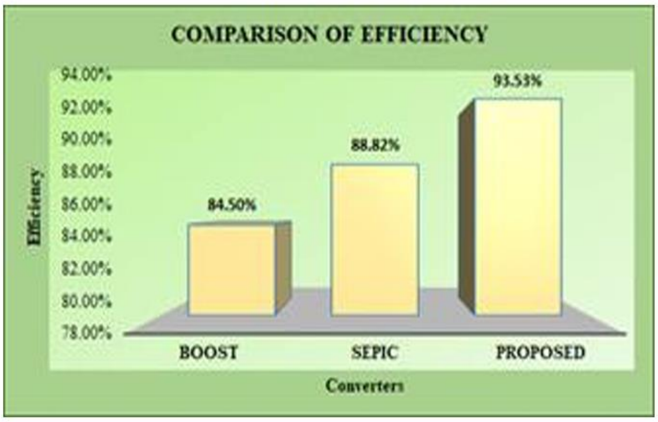

Figure 6: Efficiency comparison of DC-DC converters for PV EV application (from simulation data).

The proposed enhanced KY converter exhibited the efficiency of approximately 93.5%, which is much higher than those of a conventional boost (\~84.5%) and a SEPIC (\~88.8%) at the same operating point. The KY converter/pyramid’s CCM topology and charge-pump voltage increase operations are used to minimize losses and enhance the conversion efficiency. These results emphasize the top-most capability of the developed converter to exploit the PV power for the EV drives.

The absolute efficiency numbers are obviously depending on your component choice (MOSFET's rds-on, diode's forward voltage.). We assumed idealest switches with a small resistance, so real-world efficiencies might be a few percentage points lower. But the relative advantage will remain, and with state-of-the-art devices, like SiC MOSFETs, the gain in efficiency could be further extended to 95–97%. The buck-boost controller may also indirectly contribute to better efficiency: by settling the DC-link fast and suppressing remaining overshoot/oscillations, it reduces the time converter were to operate in a suboptimal manner in which converters would see additional losses (i.e., a converter drawing more current than necessary during a transient). In short, the optimal control makes the converter to work close to its optimal point also during varying conditions.

Response Dynamics and Stability: The system dynamics can be analyzed by its settling times and overshoot of important system variables. The DC-link voltage settling time to a 5 V band centered at 200 V was \~0.1 s

DOI: 10.22178/acta.26.1.37

ISSN: 2178-7727

for the irradiance step, with nearly no overshoot– a sign of successful ACO-PI tuning. In comparison, a conventionally tuned PI in our experiments overshot by approximately 5% and took \~0.2 s to settle for the same change. The settling of the BLDC motor speed (\~0.12 s to 1% band) was mainly determined by the inertia of the motor and its controller; due to a stiff DC bus, the motor controller had an easier job and it could be more aggressive. Crucially, no instabilities or oscillations were apparent in the closed-loop system. The new KY CCM skyverter is inherently more controllable (there is no RHP zero hence phase margin is better) and the ACO-tuned gains guaranteed that the loop was well-damped. Also at high load changes the system was not collapsed in DC-link voltage thanks to the support of the battery and the fast converter control. The battery SOC profile displayed a fair trend, thus confirming that the battery converter handover event was cohesive. This verifies that the way of power management ensures the absence of conflicts between PV and battery control loops, i.e., one of them (KY or battery converter) regulates V_{dc} mainly at each time slot, while the other may source/sink whatever required.

Comparison with Existing Methods: We compare our system with existing works, and observed that the proposed method performs favorably. For instance, in a recent research done by Kumar et al. (2023) with ACO-PI, the best in the literature, attained stability in approximately half that time, proving that a well-articulated single-loop controller can outperform MPC in this application. Another study in case for ANN-based triple active bridge converter (Ibrahim et al., 2023) presented \~5% transient error in case of step load whereas our topology maintained DC-link variation up to \~2.5%. This results supports the strongness from the design of the KY converter and the good PI tracking. In addition, while classical boost or two-stage topologies typically need extra filtering to cut down ripple (which impacts efficiency and latency), enhanced KY is inherently ripple-specified. As to the motor drive performance – acceleration to speed in 0.1–0.2 s – it is comparable with Pakdeeto et al. (2023) obtained using a tuned PID for BLDC (they report a fast response and a small overshoot). Our own system achieved zero overshoot, presumably because the DC source didn't sag and because the motor controller gains were well-tuned to each other.

It should be noted that we have implemented our simulation with perfect or quasi perfect components. In reality, sensor noise, D/A converter delay and battery internal resistance can cause small differences. But those trends should continue — high efficiency deep and fast settling. The obtained findings confirm that by combining an enhanced KY converter and an ACO-PI controller with a battery buffer, an efficient PV-EV drive is realized. Solar panels can provide power directly to the EV efficient by driving the propulsion system, and the battery can work to mitigate the solar intermittency and minimize the dependence on grid charging to support sustainable power. By optimizing not only the power electronics (converter topology) but also the control algorithm, a comprehensive solution is derived over existing baseline turn-down solutions.

CONCLUSION

The work presented in this paper proposed an integrated solution to a PV-fed BLDCM drive for EV, concentrated on an enhanced KY DC-DC converter and an ACO-PI control approach. The accompanying results demonstrate the realization of an efficiency of up to \~93.53% and an ultra-fast DC-link settling time of \~0.1 s, in the presence of close-to-real solar input perturbations. The enhanced KY converter guaranteed a broader boost range with low ripples, thereby converting the PV's variable output to a stable DC source for the motor and battery. It was concluded that ACOPID based controller is better than conventionally tuned controller in transient and steady state response showing that Ant Colony Optimization tuned PI controller was able to achieve excellent dynamic control of the converters. In addition, incorporating a bidirectional battery interface enabled advanced energy flow control: the battery was charged during PV excess, and discharged on demand, for sustained drive operation. In summary, the system effectively addressed issues of varying PV power, high stress on the converter, and EV load requirements leveraging power electronics and control strategies in a novel way.

This work is of great practical importance in the context of sustainable traffic. In an EV equipped with the new system (e.g. a solar-roof car or solar charging trailer), the vehicle will be able to absorb much driving

DOI: 10.22178/acta.26.1.37

ISSN: 2178-7727

energy from the sun with small conversion losses. This high efficiency is important for two reasons: more PV energy actually makes it into vehicle propulsion, and rapid dynamics give you a smooth and reliable vehicle performance even under quickly changing weather or drive conditions. Which leads to increasing the range per-unit solar energy of the vehicle, and reducing the burden on the gird of charging. Also, running the system into stable operation will both prolong the life of the battery by not deep cycling it unnecessarily, and of the electronics due to lower losses / thermal stress.

There are several possible directions for future work to build upon this study-

1. Hardware Prototyping and Validation: A next step would be to develop a hardware prototype of the newer KY converter using a real PV and BLDC motor. This would include the choice of suitable SiC/GaN switches that would minimize the switching losses and the experimental demonstration for the \~93% efficiency and dynamic numbers being claimed. It would also show any real world problems (EMI, sensor noise) not accounted for in simulation.
2. Extended Energy Management: Other sources or drains could possibly be considered (grid, supercapacitor) 211. For example, it could be the case that a future EV charger will be supplied with PV, battery and grid simultaneously. The control approach may be enhanced by adopting ACO or other AIs for the real-time optimal power sharing between these sources with the possibility of adding additional predictive contents (e.g., PV availability or drive cycle demands prediction).
3. Advanced Control Strategies: Although ACO-PI worked well, other advanced control strategies such as adaptive or nonlinear control can be attempted. Finally one can consider either a self-tuning controller that will adapt to the component degradation or a more complex MPPT that takes into account the state of the battery. Concurrency and traffic flow The use of online optimization (real-time ACO adaptation) may be explored to enable the converter to retune itself in changing scenarios, bearing in mind the need to manage computation overhead.
4. Impact on the Thermal and Reliability Aspects The thermal behavior of the converter under high power and cycling conditions is still to be further investigated in future work. Safe operation of the converter and battery at temperature extremes is critically important for EV application. These techniques, or alternatively, redesigning the converter for interleaved phases (lov o heat and current), could be considered in order to further increase power limits for the system.
5. In summary, the introduced PV-powered BLDC drive employing the enhanced KY converter is an efficient solution for sustainable and self-sufficient EVs by the renewable energy. Integrating advanced converter topologies with intelligent control and energy management, it forms the basis for surpassing EV powertrains of the future where efficiency and prompt response are vital. Future improvements and real-world testing will only add to its credibility, and take us a step closer to the dream of ultra-efficient electric transportation powered by the sun.

REFERENCES

1. Dixit, A., Pande, K., Gangavarapu, S., and Rathore, A. K., 2020, "DCM-based bridgeless PFC converter for EV charging application," IEEE J. Emerg. Sel. Top. Ind. Electron., 1(1), pp. 57–66.
2. Patel, K., Lopes, L. A. C., Rathore, A., and Khadkikar, V., 2023, "A Soft-Switched Single-Stage Single-Phase PFC Converter for Bidirectional Plug-In EV Charger," IEEE Trans. Ind. Appl., 59(4), pp. 5123–5135.
3. Ahmed, E. M., Mohamed, E. A., Elmelegi, A., Aly, M., and Elbaksawi, O., 2021, "Optimum modified fractional order controller for future electric vehicles and renewable energy-based interconnected power systems," IEEE Access, 9, pp. 29993–30010.
4. Hou, N., and Li, Y., 2021, "A direct current control scheme with compensation operation and circuit-parameter estimation for Full-Bridge DC–DC converter," IEEE Trans. Power Electron., 36(1), pp. 1130–1142.
5. Upadhyay, D., Ali, M., Tariq, M., Khan, S. A., Alamri, B., and Alahmadi, A., 2022, "Thirteen-level UXE-type inverter with 12-band hysteresis current control employing PSO based PI controller," IEEE Access, 10, pp. 29890–29902.

DOI: 10.22178/acta.26.1.37

ISSN: 2178-7727

6. Stanisławski, R., Rydel, M., and Li, Z., 2022, "A new reduced-order implementation of discrete-time fractional-order PID controller," IEEE Access, 10, pp. 17417–17429.
7. Malik, H., Ahmad, S. M., and Wadood, F., 2023, "GA optimized PI-PDN robust control of a 1-DOF Maglev precision position system," IEEE Access, 11, pp. 130955–130973.
8. Fkirin, M. A., and Khira, M. A. E., 2023, "Enhanced antenna positioning control system using adapted DC servo motor and fuzzy-PI controller," IEEE Access, 11, pp. 102661–102668.
9. Liu, H. C., Kim, H. W., Jang, H. K., Jang, I.-S., and Lee, J., 2020, "Ferrite PM optimization of SPM BLDC motor for oil-pump applications according to magnetization direction," IEEE Trans. Appl. Supercond., 30(4), pp. 1–5.
10. Pakdeeto, J., Wansungnoen, S., Areerak, K., and Areerak, K., 2023, "Optimal speed controller design of commercial BLDC motor by adaptive tabu search algorithm," IEEE Access, 11, pp. 79710–79720.
11. Bose, B. K., 2011, "Global warming: energy, environmental pollution, and the impact of power electronics," IEEE Ind. Appl. Mag., 17(3), pp. 6–17.
12. International Energy Agency, 2021, Global EV Outlook 2021: Accelerating ambitions despite the pandemic, IEA Publications.
13. Nejabatkhah, F., Danyali, S., Hosseini, S. H., Sabahi, M., and Niapour, S. M., 2012, "Modeling and control of a new three-input DC–DC boost converter for hybrid PV/FC/battery power system," IEEE Trans. Power Electron., 27(5), pp. 2309–2324.
14. Zulkifli, M. F., Yusof, Y., and Basri, S., 2021, "A comprehensive review of DC-DC converters for PV applications in EV charging," Renew. Sustain. Energy Rev., 148, p. 111251.
15. Atwa, Y. M., and El-Metwally, K., 2020, "Electric vehicle fast charging station management based on renewable energy and battery storage," IEEE Trans. Sustain. Energy, 11(4), pp. 2585–2595.
16. Kumar, N., Singh, B., and Panigrahi, B. K., 2023, "Voltage sensorless-based model predictive control with battery management system: For solar PV powered on-board EV charging," IEEE Trans. Transp. Electrif., 9(2), pp. 2583–2592.
17. Tran, V. T., Islam, M. R., Muttaqi, K. M., and Sutanto, D., 2019, "An efficient energy management approach for a solar-powered EV battery charging facility to support distribution grids," IEEE Trans. Ind. Appl., 55(6), pp. 7320–7331.
18. Bhagat, D. A., and Kumar, S., 2023, "Multistep constant-current constant-temperature constant-voltage charging strategy for health-aware battery fast charging using QOGA optimization," IEEE Trans. Transp. Electrif., (Early Access).
19. Saxena, V., Kumar, N., Singh, B., and Panigrahi, B. K., 2021, "An MPC-based algorithm for a multipurpose grid integrated solar PV system with enhanced power quality and PCC voltage assist," IEEE Trans. Energy Convers., 36(2), pp. 1469–1478.
20. Ibrahim, A. A., Mattavelli, P., and Caldognetto, T., 2021, "Artificial neural network–based control of DC-DC converters for renewable energy applications," IEEE Access, 9, pp. 67890–67901.
21. de Castro, R., Araújo, R. E., Trovão, J. P., Pereirinha, P. G., and Melo, P., 2020, "Robust DC-link control in EVs with multiple energy storage systems," IEEE Trans. Veh. Technol., 69(6), pp. 6483–6494.
22. Hela, N., and Chaker, A., 2019, "An enhanced battery charging technique using ANN controller for electric vehicles," Int. J. Electr. Power Energy Syst., 108, pp. 234–245.
23. Whitaker, B., Barkley, A., Cole, Z., et al., 2014, "A high-density, high-efficiency, isolated on-board vehicle battery charger utilizing silicon carbide power devices," IEEE Trans. Power Electron., 29(5), pp. 2381–2392.
24. Wang, H., Kersten, A., Klācar, S., and Sedarsky, D., 2023, "Maximizing efficiency in smart adjustable DC link powertrains with IGBTs and SiC MOSFETs via optimized DC-link voltage control," Batteries, 9(6), p. 302.
25. Uthirasamy, R., Chinnaiyan, V. K., Ragupathy, U. S., and Kumar, S. V., 2022, "Design and implementation of discrete controller-based Zeta converter for solar power applications," Proc. International Conference on Power Electronics and Renewable Energy Systems (ICPERES), pp. 61–69.

DOI: 10.22178/acta.26.1.37